Journal of
Ship&Ocean
Technology
©SEPTEMBER 2008

SOTECH Vol. 12, No. 3, pp. 36 ~ 54, 2008

A Numerical Study on the Geometry of Jet Injection Nozzle of a Coanda Control Surface

Dae Won Seo[1], Jong Hyun Kim[1], Hyochul Kim[2] and Seung-Hee Lee[1]

[1] Department of Naval Architecture and Ocean Engineering, Inha University, Inchoen, Korea

[2] Jungseok Research Institute of International Logistics and Trade, Inha University, Inchoen, Korea;
Corresponding Author: shlee@inha.ac.kr

Abstract

A jet stream applied tangential to a curved surface in fluid increases lift force by strengthening circulation around the surface and this phenomenon is known as the Coanda effect. Many experimental and numerical studies have been performed on the Coanda effect and the results found to be useful in various fields of aerodynamics. Recently, preliminary studies on Coanda control surface are in progress to look for practical application in marine hydrodynamics since various control surfaces are used to control behaviors of ships and offshore structures.

In the present study, the performance of a Coanda control surface with different geometries of the jet injection nozzle was surveyed to assess applicability to ship rudders. A numerical simulation was carried out to study flow characteristics around a section of a horn type rudder subjected to a tangential jet stream. The RANS equations, discretized by a cell-centered finite volume method were used for this computation after verification by comparing to the experimental data available. Special attentions have been given to the sensitivity of the lift performance of a Coanda rudder to the location of the slit (outlet) and intake of the gap between the horn and rudder surface at the various angles of attack. It is found that the location of the water intake is important in enhancing the lift because the gap functions as a conduit of nozzle generating a jet sheet on the rudder surface.

Keywords: Coanda effect, Coanda rudder, jet injection nozzle, jet slit

1 Introduction

The Coanda effect, discovered by Henry Coanda, is a physical phenomenon which has been applied to various fields in aerodynamics (Lee et al 2007). The Coanda effect demonstrates that a flow tangential to a solid surface generates low-pressure fields around it and consequently the flow remains tangential even along the curved surface as far as the pressure force surpass the centrifugal force of the flow turning about the surface.

Many studies on the Coanda effect that have been carried out so far focus on the spiral jet type. The effect of the gap clearance of jet injection slit and the local curvature of the surface at the slit have been carefully surveyed by Horri, K. et al (1991). Studies also have

been carried out on the effect of the jet blowing angle to the surface at the slit (Matsuo et al 2003, Horri, K. et al 1991)

The conventional practice of installing rudders downstream of propeller may not guarantee sufficient rudder force for proper maneuvering of a ship at low speeds. In previous studies, variation of the cross sectional shape of a rudder and addition of appendages have been investigated to improve the rudder performance (Seo et al 2007). In other studies, water jet has been injected tangentially over rudder surfaces with or without a flap to enhance the rudder force by the resulting Coanda effect (Park and Lee 2000, Rhee et al 2003, Ahn and Kim 2003).

In the present paper, the proper locations of the slit and water intake of the gap between the horn and rudder surface have been numerically surveyed to support a design of Coanda rudder. For verification of the numerical method, the results were compared to the existing experiment (Englar, 1971). In the process, the sensitivity of the numerical solution to the turbulence models and the grid sizes were also examined. After then, the hydrodynamic performance of the Coanda rudder section has been numerically investigated for the various locations of the slit and intake of the gap between the horn and rudder. The effects of tip vortex and Reynolds number were also studied for verification of experimental setup under consideration and for possible use in interpretation of the result.

2 Computational methods

2.1 Governing equations

A numerical study was carried out using FLUENT, a general purpose commercial software. The governing equations are written for the mass and momentum conservation, such that

$$\frac{\partial \rho}{\partial t} + \nabla \cdot \left(\rho \vec{v} \right) = 0 \tag{1}$$

$$\frac{\partial}{\partial t}\left(\rho \vec{v} \right) + \nabla \cdot \left(\rho \vec{v} \vec{v} \right) = -\nabla p + \nabla \cdot \left(\overline{\tau} \right) \tag{2}$$

where $\vec{v}$ is the velocity vector in the Cartesian coordinate system, p is the static pressure, and $\overline{\tau}$ is the stress tensor given by

$$\overline{\tau} \equiv \mu \left[\left(\nabla \vec{v} + \nabla \vec{v}^{T} \right) - \frac{2}{3} \nabla \cdot \vec{v} I \right] \tag{3}$$

where μ is the molecular viscosity, I is the unit tensor, and the second term on the right hand side is the effect of volume dilation. Following the application of the Reynolds averaging approach for turbulence modeling, the Navier-Stokes equations can be written in Cartesian tensor form as

$$\frac{\partial \rho}{\partial t} + \frac{\partial}{\partial x_i} \cdot \left(\rho u_i \right) = 0 \tag{4}$$

$$\frac{\partial}{\partial t}\left(\rho u_i \right) + \frac{\partial}{\partial x_i}\left(\rho u_i u_j \right)$$

$$= -\frac{\partial p}{\partial x_i} + \frac{\partial}{\partial x_j}\left[\mu\left(\frac{\partial u_i}{\partial x_i} + \frac{\partial u_j}{\partial x_i} - \frac{2}{3}\delta_{ij}\frac{\partial u_l}{\partial x_l}\right)\right] + \frac{\partial}{\partial x_j}\left(-\rho\overline{u_i' u_j'}\right) \tag{5}$$

where δ_{ij} is the Kronecker delta, and $-\rho\overline{u_i' u_j'}$ represents the Reynolds stresses. These Reynolds stresses must be modeled in order to close Eq. (5), i.e. for turbulence closure.

2.2 Turbulence models

The $k-w$ SST (Menter, 1994), $k-w$ model hereafter, and Reynolds stress transport turbulence models (Launder and Shima, 1989), RSTM hereafter, are used for turbulence closure in the present study. The $k-w$ model is one of the most widely used turbulence models for external flow in aero- and hydrodynamics. RSTM is the most advanced turbulence model for engineering applications and has better potential over other models in predicting the essential features of the turbulent flow. The detailed implementation of the models into the present numerical code is described in Kim (2001) and Kim et al.(2002)

2.3 Numerical schemes

The numerical approach used in the present study employs a cell-centered finite-volume method along with a linear reconstruction scheme that allows the use of computational cells with arbitrary polyhedral shapes. Convection terms are discretized by a second order accurate upwind scheme, while diffusion terms by a second order accurate central differencing scheme. For transient flow calculations, time derivative terms are discretized by a first order backward implicit scheme. The velocity-pressure coupling and overall solution procedure are based on a SIMPLE type segregated algorithm adapted to an unstructured grid. The discretized equations are solved using point wise Gauss-Seidel iterations, while the algebraic multi-grid method accelerates the solution convergence. The relaxation factors are set to be 0.3 for pressure, 0.5 for momentum, and 0.5 for turbulence.

3 Numerical calculations

3.1 Two-dimensional elliptic foil

While the calculation scheme is important when performing numerical simulations, the selection of an appropriate turbulence model and grid composition for calculation quality has more effect on the analysis results (Wilcox 1993).

In this study, various turbulence models and grid compositions have been examined to find whether it can accurately express the flow in the boundary layer near the surface of the Coanda surface. Numerical computation on the flow field around the 2-dimensional Coanda elliptic foil have been carried out in accordance with the data used in the experiment by Englar (1971) as given in Table 1. The results of computations have been compared to verify with the experimental results of Englar.

Table 1: Major parameters of the computation for 2-dimensional elliptic foil (Englar, 1971)

Chord (C)	0.2032m
Aspect ratio	0.15
Angle of attack	3°
Slit height (h)	0.00125c at 0.924 C
Jet momentum coeff. (C_j)	0.138
Mass flow rate	0.084kg/s
Infinite velocity	3 9.4m/s

The computation domain for the elliptic foil extends to $-7 \leqq x/c \leqq 10$, $-7 \leqq y/c \leqq 7$, and the total number of grids is 48,320, as shown in Figure 1.

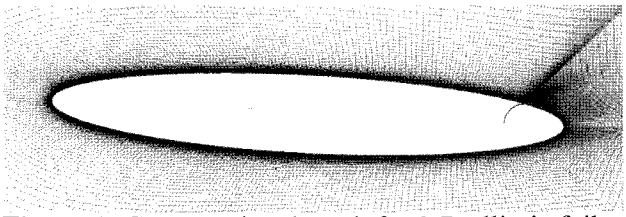

Figure 1: Computational mesh for 2-D elliptic foil

To examine the influence of a turbulence model and grid dependency, calculations have been performed on a total of 9 cases. Typically, the k-ε turbulence model that uses the wall function requires the first node to be placed within the range of $30 < y^+ < 300$ from the surface. However, the k-ω and RSTM models that do not use the wall function require stricter condition in that the first node should be placed within $y^+ < 10$. In the present calculations, y^+ are set to be less than 70 for k-ε model and less than 10 for k-ω and RSTM models.

3.2 Effect of the jet injection conduit arrangement

Figure 2 shows a section of the Coanda rudder modified from a rudder section of a bulk carrier to exploit the gap between horn and rudder surface as a conduit of jet nozzle for generating Coanda effect. The section of the rudder is based on NACA0020 and the chord and span is determined as 6.25 m and 12.5 m, respectively, considering the typical rudder dimension of bulk carriers. If a 1/25 scale model is to be used in experiments, the chord of the model will be 0.25 m and the span 0.5 m. Similarly the opening clearance of the pressurized water intake is set to be 1mm, and the gap clearance between horn and rudder surface as 0.85 mm by considering the practical manufacturing margin of rudder under consideration. As usual, the horn of the rudder is fixed in line with the center plane of a ship while the rudder surface rotates about the pintle shaft. The pintle shaft is hollow and intakes are pierced perpendicular to the center plane of ship as shown in Figure 2. A

Cartesian coordinates system with origin at the centerline of the pintle shaft and x-axis parallel to the center plane has been used as shown in the figure. The figure also shows a concentric tube with partial opening is inserted in the shaft to work as a valve system directing the jet flow to suction side at any rudder angle.

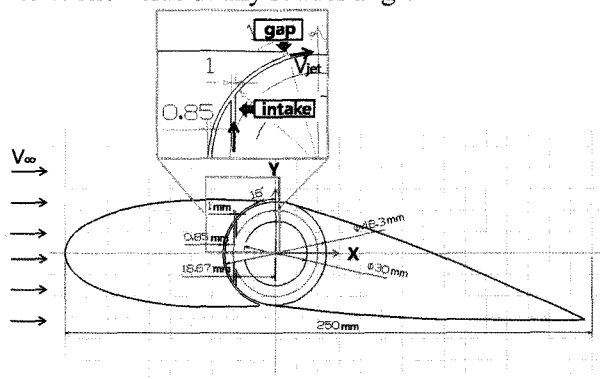

Figure 2: Schematic diagram of jet nozzle device

Specific dimensions of the Coanda rudder and conditions for the experiment in preparation are summarized in Table 2.

Table 2: Principal dimensions of the scale model of the Coanda rudder

Scale	25:1
Chord	0.25 *m*
Span	0.5 *m*
Maximum thickness	0.05 *m*
h (slit height)	0.85 *mm*
H (jet intake opening)	1 *mm*

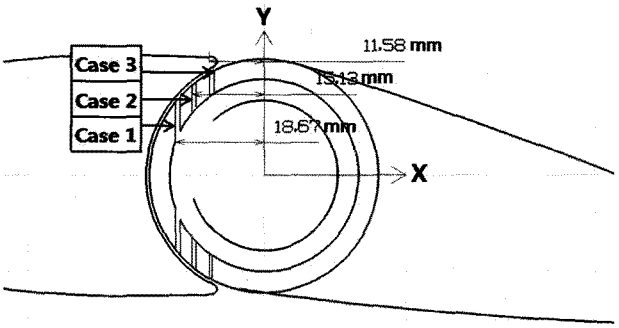

Figure 3: Various locations of the jet intake

The flow fields around a rudder section were numerically calculated at the various locations of jet intake and slit. The optimum points of the intake and slit were selected among the results at three different locations each.

Three different positions of the intake were considered to examine influence of the intake location on the lift performance. The distance (d) between the centerline of the pintle and

jet intake along x-axis for cases 1, 2, and 3 is 18.67 *mm*, 15.13 *mm*, and 11.58 *mm*, respectively, as shown in figure 3. For the cases, the computational grid has the identical C-type topology, and a total number of 45,000 grids were used. The RSTM was selected in accordance with the results of the verification reported in section 3.1 and y^+ of the first node was kept less than 1 in all the computation. The calculations were performed at the rudder angles (angles of attack) of 0°, 6°, and 12°.

Three different locations of jet slits, case 1, 2 and 3, as shown in Figure 4 were also tested. The location of the jet slit needs to be optimized since it determines the angle of jet flow relative to the rudder surface and eventually affects the flow characteristics along the surface significantly.

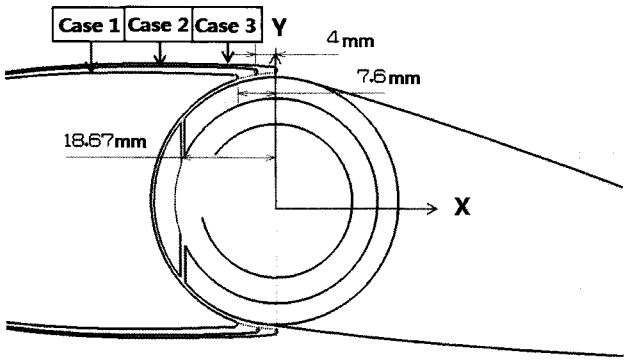

Figure 4: Various positions of the jet slit and difference in horn shape

The distance (D) of the horn trailing edge form the pintle center along the x-axis is 7.6 *mm*, 4 *mm* and 0 *mm* for case 1, 2 and 3, respectively. The extension of the horn trailing edge inevitably changes the shape of the horn section also if the slit height kept constant as shown in the figure. The maximum thickness of the horn increases 5% and 7% in case 2 and 3 comparing to case 1.

All the calculation was performed with jet momentum coefficient of 0.2, as shown in Table 3, where the jet momentum coefficient is defined as

$$C_j = \frac{\dot{m} V_{jet}}{\frac{1}{2}\rho V_\infty^2 C} \tag{6}$$

Here, $\dot{m}$ refers to mass flux (kg/s), V_{jet} refers to the average speed of flow that ejects through the slit, and ρ, V_∞ refers to the density and speed of the incoming flow. The influence of the propeller has not been considered in the computation and the speed of inflow has been fixed at 0.507m/s and the speed of jet at 2.75m/s.

3.3 Three- dimensional effect

With the most effective rudder section found in the previous section, a three-dimensional analysis was carried out at the conditions shown in Table 3..

Table 3: Conditions for 3-D computation

C_j	0.2
V_∞	0.507 *m/s*
V_{jet}	2.750 *m/s*
Jet flux	0.0017 m^3/s

The composition of the computational grids for the three dimensional rudder was carried out with Gridgen ver. 15.08. The grid is a C-H type, and the number of surface grids equals 151 by 59 on the each side of rudder surface and 11 across the gap between the horn and the rudder surface as shown in Figure 5

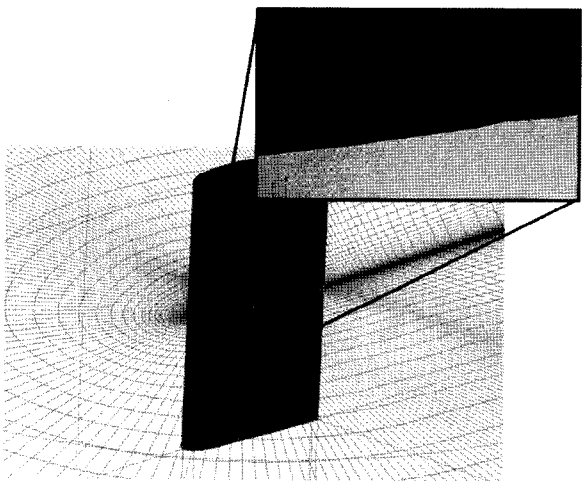

Figure 5: Computational mesh for 3-D coanda foil

The calculation domain was extended to $-4 \leqq x/C \leqq 7$, $-4 \leqq y/C \leqq 4$, and $0 \leqq z/C \leqq 4$ and

the total number of the grids used in the computation is about 880,000. The k-ω turbulence model was used in the computation since the RSTM model consumes an excessive computational resource.

4 Results

4.1 Two-dimensional elliptic foil

In the computations, 250 grid points on the surface of the ellipse and 15 points across the Coanda slit were distributed and influence of $y+$ value and turbulence model on the accuracy of numerical solution was studied. The results for the are provided in Table 4.

Table 4: Comparison of C_L for the various turbulence models and grid qualities at the angle of attack $\alpha=3°$.

C_L	1.944

Case	No. of grid point on	Y+	Turbulence Model	C_L	C_L error(%)
1	250, 15	Y+<70	k-ε	2.12	9.05%
2-1	250, 15	Y+<10	k-ω	2.06	5.97%
2-2	250, 15	Y+<10	RSTM	1.83	5.86%
3-1	250,15	Y+<3	k-ω	2.05	5.45%
3-2	250, 15	Y+<3	RSTM	1.86	4.32%
4-1	250, 15	Y+<1	k-ω	2.02	3.91%
4-2	250, 15	Y+<1	RSTM	1.87	3.81%
5-1	425, 20	Y+<1	k-ω	1.98	1.85%
5-2	425, 20	Y+<1	RSTM	1.931	0.67%

A standard k-ε model with wall function was used in case 1 and lift was over estimated more than 9% of the experimental one. Hence, the RSTM and k-ω turbulence models were selected and corresponding numerical solutions were compared with the experiment at various y^+ as shown in the table in cases 2-1 through 4-2. The results for RSTM model fitted the experiment more close than the k-ω model in general but overall accuracies were not quite satisfactory. Thus, the number of grid points on the foil surface was increased to 425 and 20 points were used across the jet slit in case 5-1 and 5-2 while keeping y^+ less than 1. Then, the computed lift coefficient of case 5-2 with RSTM showed better coincidence than the result with k-ω to match 99.3% of the experiment.

Figure 6 compares the calculated pressure distributions with the experiment of Englar in terms of the various turbulence models and grid qualities. It is shown in the figure that computed pressure distribution for case 5-2 matches most closely with the value found in the experiment.

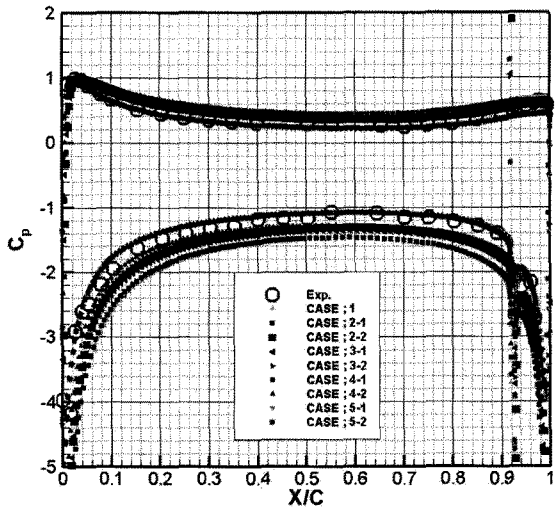

Figure 6: Comparison of surface pressure distributions of 2-D foil computed from various turbulence models

Figure 7 shows the velocity magnitude of the flow field for case 5-2, fits the most with the experiment. It can be verified that the jet flow ejects from the slit successfully follows the foil surface to achieve increase in circulation.

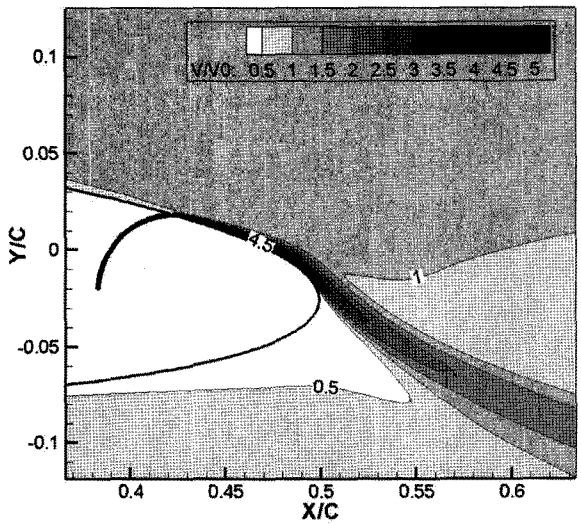

Figure 7: Distribution of velocity magnitude of Case 5-2 (RSTM, grid points;425, 20)

4.2 Effect of slit location

Figure 8 compares the lift coefficients of the Coanda surface at various locations of the slit. In case 3, when the trailing edge of the horn is the closest to the y-axis, the lift is maximized to have 7~8% increase comparing to case 1 at the angles of attack of 6° and 12°. This is because the location of the slit in case 3 is designed to allow the jet flow flows more tangential to the rudder surface by adjusting the jet incident angle to the surface. However, it is difficult to extend the trailing edge of the horn to the closest location when designing a practical rudder. Therefore, D=6.5mm, a point between the edge locations of case

1 and 2, has been selected to keep the slit height constant on the both sides even at the maximum rudder angle of 35°.

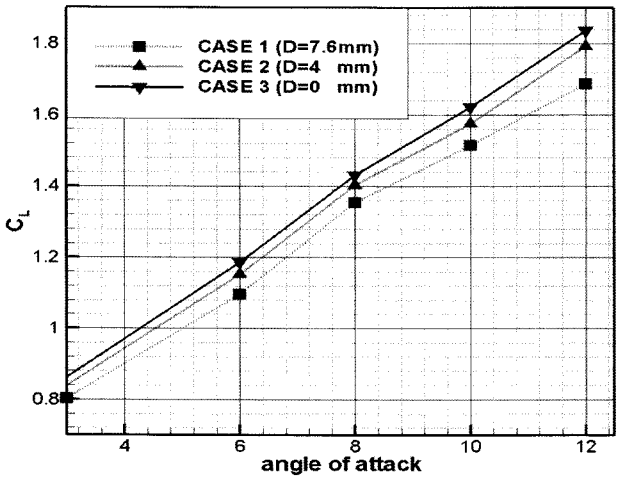

Figure 8: Comparison of lift coefficient for the various locations of the jet slit and angles of attack

Figure 9 presents the velocity magnitude contour on the suction side of the cross section for the various locations of the jet slit. It can be seen that in case 2 and 3, the jet flow successfully follows the surface of the rudder section (Figure 9b, c). Although case 1 (*D*=7.6 *mm*) shows profound region of retarded flow near the slit comparing to the other cases

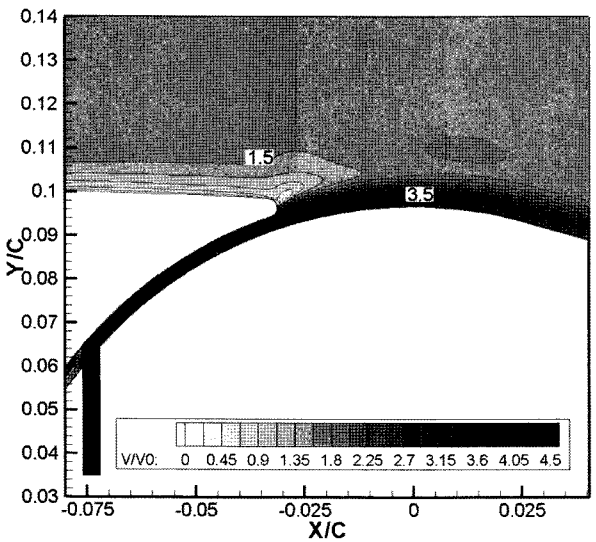

(a) Case 1 (*D*=7.6 *mm*)

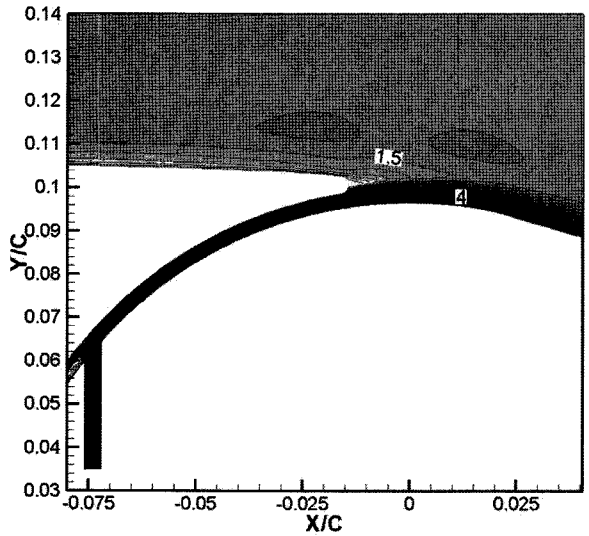

(b) Case 2 (D=4 *mm*)

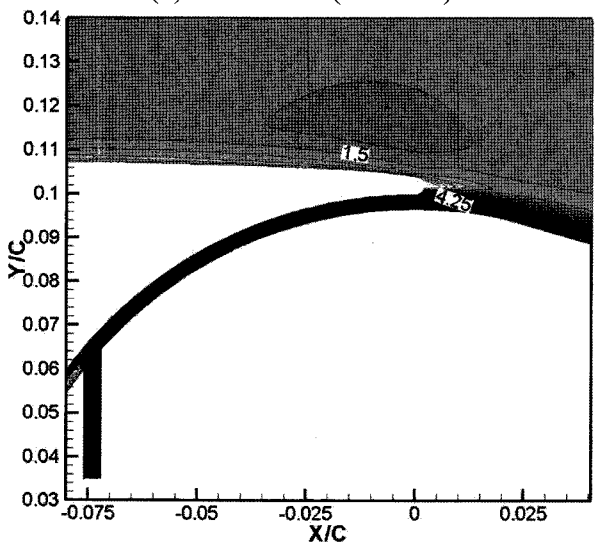

(C) Case 3 (D=0 *mm*)

Figure 9: Contour of velocity magnitude at the various slit locations (C_j=0.2, α=12° d=18.67*mm*)

4.3 Effect of intake location

Figure 11(a) ~ (c) present the distributions of velocity magnitude around the nozzle at the various locations of jet intake. Figure 11(a) shows that, in case 1, the jet flow follows the surface better than the flow when the location of intake moves closer to the slit(case 2, 3) as shown in Figure 11(b, c). Thus it can be presumed within the scope of present work that better performance can be achieved by placing the jet intake at the location furthest away from the slit so as to maximize the length of the jet nozzle conduit. It is also found that if the conduit length is not sufficient, a portion of the flow from the intake escapes to the pressure side of the rudder and consequently diminishes the lift.

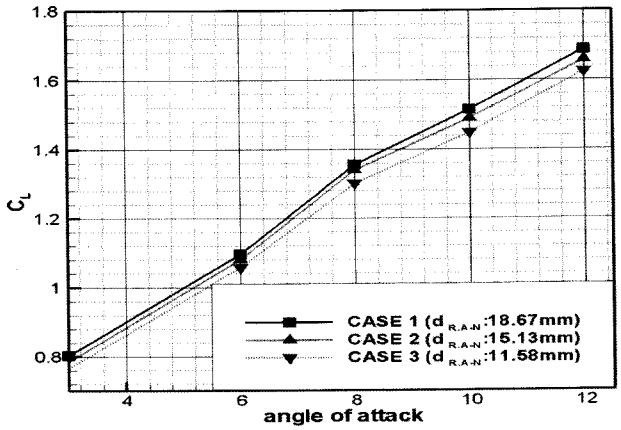

Figure 10: Comparison of lift coefficients for the various locations of the jet intake and angles of attack

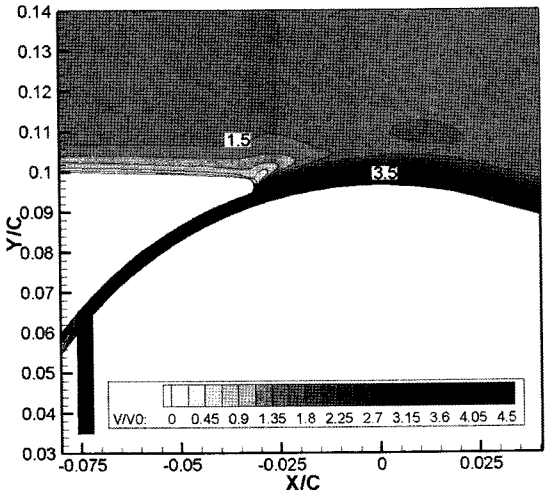

(a) Case 1 (d=18.67mm)

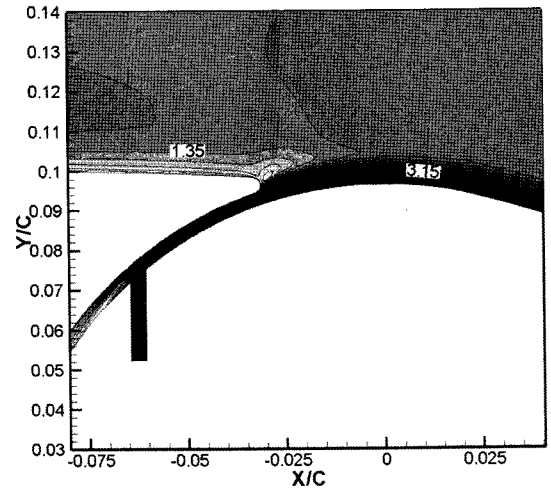

(b) Case 2 (d=15.13 mm)

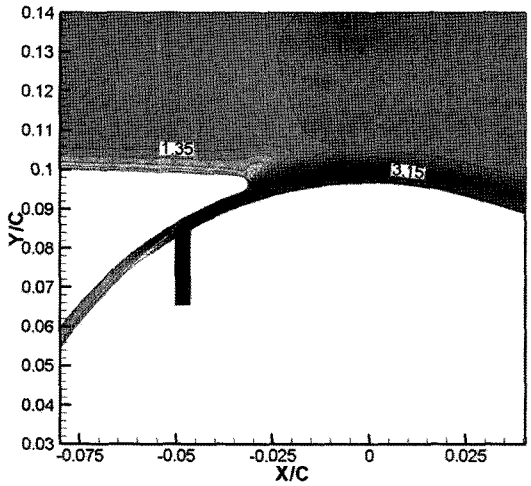

(c) Case 3 (d=11.58 *mm*)

Figure 11: Contour of velocity magnitude for various intake location (C_j=0.2, α=12°, D=6.5*mm*)

4.4 Three -dimensional effect.

In accordance with the results obtained from the flow analyses outlined in the previous section, the locations of the jet intake and slit for the scale model of Coanda rudder have been determined.

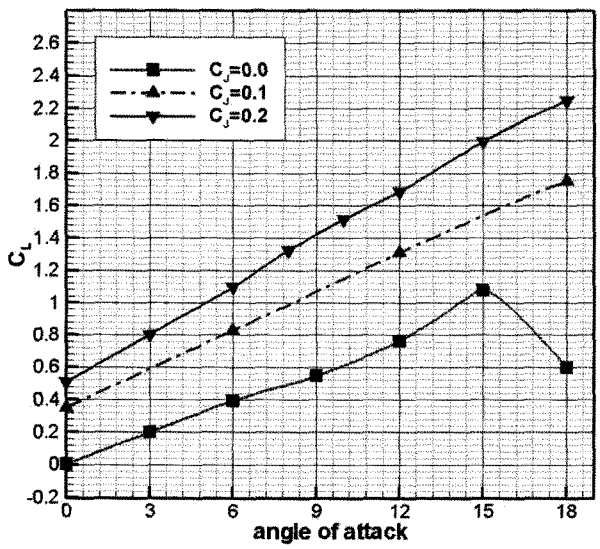

Figure 12: Comparison of lift coefficient of Coanda surface for various C_j

Figure 12 presents 2-dimensional lift performance of the Coanda rudder in terms of the jet momentum coefficient C_j and angle of attack. It can be seen that a stall occurs as expected at the angle of attack around 15° when jet is not injected but the lift continues to increase above the angle after jet applied. The lift improves up to 70% and 120% at the angle of attack of 12° with jet momentum coefficients of 0.1 and 0.2, respectively.

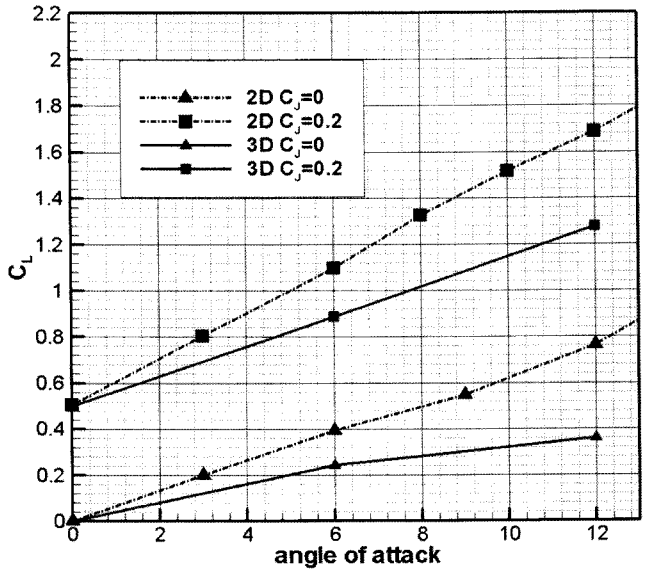

Figure 13: Comparison of lift coefficient of Coanda rudder for various angles of attack

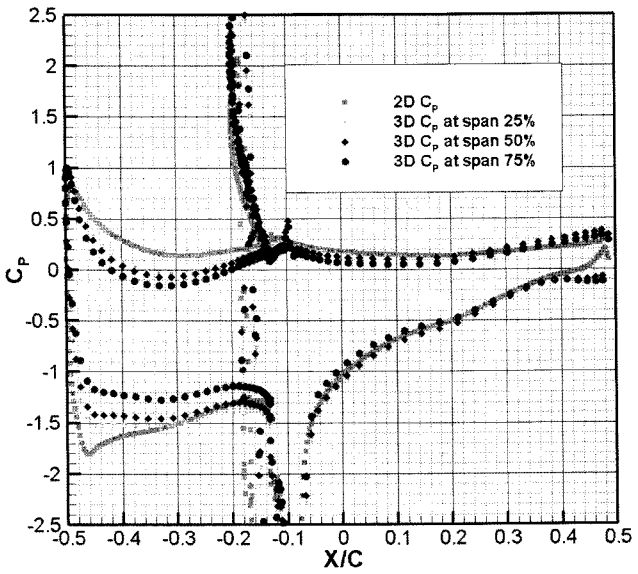

Figure 14: C_p distribution on the various cross sections of Coanda rudder (α=12°, C_j =0.2)

Figure 13 compares the computed lifts of the Coanda rudder of uniform cross section at the jet momentum coefficient C_j = 0.2. The results are compared with the 2-D results in the figure to show up to 32% diminution of the lift due to the presence of tip vortex of finite lifting foils. Figure 14 shows the surface pressure distributions of the cross sections at the different span wise locations and the decrease in the sectional lift become apparent as the section situates closer to the tip.

4.5 The scale effect

The influence of the Reynolds number on the Coanda effect has been examined to verify the experimental set up. Calculations have been performed at jet momentum coefficient C_j of 0.1 and 0.2 and three different chord-based Reynolds number, $R_n = V_\infty C/\nu$, where ν is the kinematic viscosity, C chord length and V_∞ incoming velocity as shown in Table 5.

Table 5: Conditions for computation of the scale effect

V_∞ (m/s)		0.507	1.5	2.5
R_n		1.3×10^5	3.8×10^5	6.3×10^5
V_{jet} (m/s)	$C_j = 0.1$	1.944,	5.752,	9.587,
	$C_j = 0.2$	2.337	6.915	13.558

Figure 15 shows a comparison of the lift at the three different Reynolds numbers. At the lowest Reynolds number of 1.3×10^5, the lift was almost 10% lower than those for two other cases.

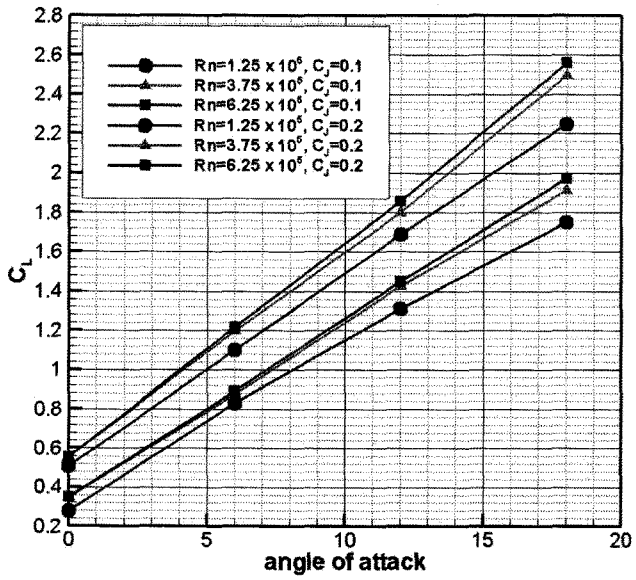

Figure 15: Comparison of lift coefficients for different R_n at various angles of attack (d=18.67mm, D=6.5mm)

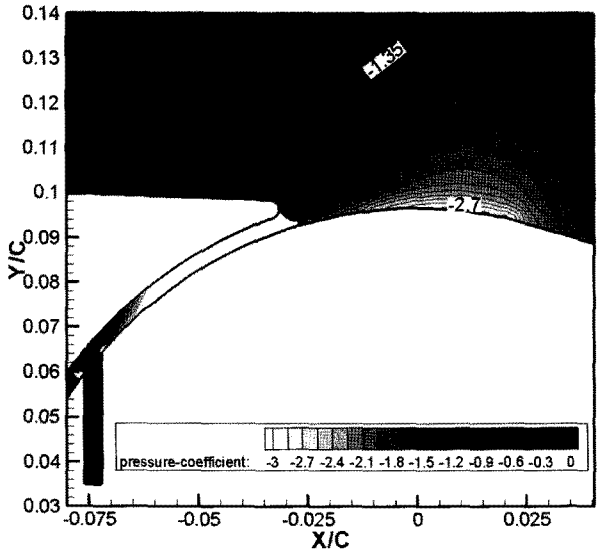

(a) Case 1 ($R_n = 1.3\times10^5$)

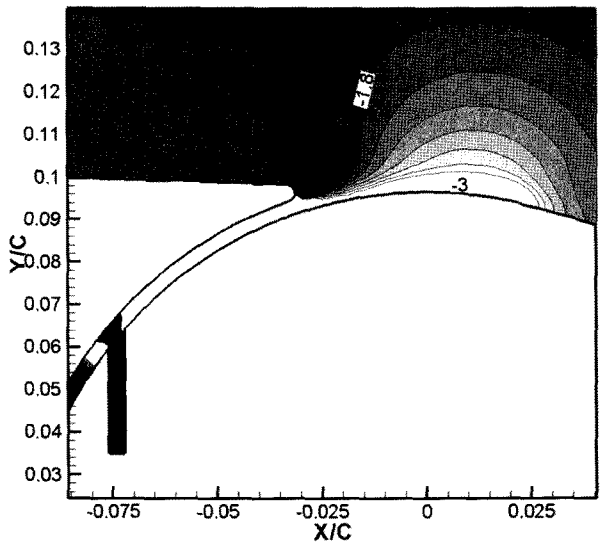

(b) Case 2 ($R_n = 3.8\times10^5$)

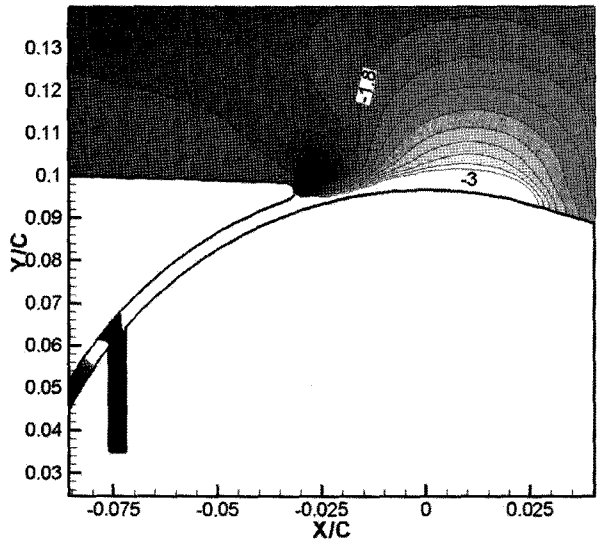

(c) Case 3 ($R_n = 6.3\times10^5$)

Figure 16: Pressure distribution at different Reynolds numbers (α=12°, C_j=0.2, d=18.67*mm*, D=6.5*mm*)

Figure 16 shows the flow characteristics in vicinity of the slit when C_j=0.2, d=18.67*mm*, and D=6.5*mm*. Figure 16(a) illustrates that at a low Reynolds number, a low lift is assumed because the flow is retarded by the viscosity near the slits. However, at a Reynolds number of 3.8×10^5 and higher, there is no significant change in the lift, even though the Reynolds number increases to 6.3×10^5. Thus, when performing an experiment on the Coanda rudder model, it is recommended that the Reynolds' number be set at 3.8×10^5 and higher in order to reduce the scale effect, although exact limit of the Reynolds number was not sought in the present study.

5 Conclusions

The effect of the jet intake and slit locations on the lift performance of the Coanda surface has been numerically studied for the purpose of finding proper configuration of jet injection nozzle of the Coanda rudder. The results are as follow:

The influence of the turbulence model and the dependency on the grid has been examined comparing with experimental data for a simple 2-dimensional case. It is found that the Reynolds Stress Turbulence Model shows the best match among others.

Considerable improvements in the lift force of a Coanda rudder have been obtained with adjustment of the slit and intake location. The lift performance was enhanced as the jet intake is placed further away from the slit and length of the jet nozzle conduit increases. Location of the jet slit is found to be also important for the lift performance of the Coanda rudder by affecting relative direction of the jet flow injection.

The flow inside the nozzle conduit is sensitive to the Reynolds number and scale effect should be carefully monitored in model tests. It is also found that tip vortices diminish the lift of the Coanda rudder considerably and that measures for avoidance of excessive tip vortex necessary.

Detail investigation on the lift performance of Coanda rudder is necessary before practical design of the rudder. Accordingly, more insight into the characteristics of the Coanda rudder will be gained upon completion of the model tests in preparation. A study is also necessary to develop a Coanda rudder with non uniform cross section.

Acknowledgements

This work was supported by the Korea Science and Engineering Foundation (KOSEF) grant funded by the Korea government (MEST) (No. ROA-2007-000-10028-0)

References

Ahn, H,-S., Kim, H., 2003, An Experimental Study of Coanda Effect on the Flapped Control Surfaces, J. of SNAK, 40, 5, pp.10-16.

Ahn, H.-S., Kim, H., 1999, Experimental Study on the Effects of Water Jetting on a Flapped Rudder, J. of SNAK, 36, 1, pp.22-29.

Englar, R, J., 1971, Two-dimensional subsonic wind tunnel tests of two 15-percent thick circulation control airfoils, David Taylor Naval Ship Research and Development Center, technical note AL-211

FLUENT 6.1 user's guide volume2 (2000)

Horii, K., Ohsumi, K., Matsma, e Y., Cheng, X. M., Tae, M. Yasukawa, E. and Hashimoto, B., 1991, A Conada Spiral Device Passing Optical Cords with Mechanical Connectors Attached Through a Pipeline, ASME Gas-Solid Flow, FED, 121, pp. 65-70.

Horri, K., Matsumae, Y., Cheng, X., M., Takei, M., Yasukawa, E. and Hashimoto, B., 1991, Focusing Phenomenon and Stability of Spiral-Flow jet, Tans. Jpn. Soc. Aeronautical and Space Science, 33, 102, pp 141-153.

Kamei,O. and Setoguchi, T., 2005, A Study on the Spiral Flow by a Coanda Nozzle, Master's Thesis, Sega University, Japan.

Kim, S.-E., 2001, Unstructured mesh based Reynolds stress transport modeling of complex turbulent shear flows, J. of AIAA paper 2001-0728.

Kim, S.-E., Rhee, S.H., 2002, Assessment of eight turbulence models for a three-dimensional boundary layer involving crossflow and streamwise vortices, J. of AIAA paper, 2002-0852

Lee, D, W., Lee, S., Kim, B, J., Kwon, S, B., 2007, A Study on Jet Characteristic using a Coanda Effect in a Constant Expansion Rate Nozzle, J. of KSAS, 35, 8, pp. 706-713

Launder, B.E., Shima, N., 1989. Second-moment closure for the near-wall sublayer: development and application. J. of AIAA, 27, 10, pp. 1319-1325

Matsuo, S., Lee, K. H.,Oda, S., Setoguchi, T. and Kim. D., 2003, Effect of Annular Slit Geometry on Characteristics of Spiral Jet, J. of Thermal Science, 12, 3, pp. 225-230.

Menter, F.R., 1994, Two-equation eddy-viscosity turbulence models for engineering applications , J. of AIAA, 32, 8, pp. 1598-1605

Park, J, J., Lee, S-H., 2000, A Numerical Study on a Circulation Control Foil using Coanda Effect, J. of SNAK, 37, 2, pp.70-76.

Seo, D, W., Jeong, S,-W., Lee, S,-H., 2007, Influence of Tail Blades on the Performance of a Fin, J. of SNAK, 44, 2, pp 55-63.

Seok-Jin Hong and Seung-Hee Lee, 2004, A Study on the Flow Characteristics around a Conada Control Surface, SOTECH, 8, 2,pp13~19.

S.H. Rhee, S.-E. Kim, H. Ahn, J. Oh, H. Kim, 2003, Analysis of a jet-controlled high-lift hydrofoil with a flap, J. of Ocean engineering, pp. 2117-2136.

Wilcox, D. C., 1993, Turbulence Modeling for CFD, DCW industries.